ACS OMEGA

Open Access

http://pubs.acs.org/journal/acsodf

Article

Preclinical Evaluation of JAB-2485, a Potent AURKA Inhibitor with High Selectivity and Favorable Pharmacokinetic Properties

Guiqun Yang, Yiwei Lin, Xin Sun, Dai Cheng, Haijun Li, Shizong Hu, Mingming Chen, Yinxiang Wang, and Yanping Wang*

Cite This: *ACS Omega* 2024, 9, 21416−21425

Read Online

ACCESS | Metrics & More | Article Recommendations | Supporting Information

ABSTRACT: As a critical mitotic regulator, Aurora kinase A (AURKA) is aberrantly activated in a wide range of cancers. Therapeutic targeting of AUKRA is a promising strategy for the treatment of solid tumors. In this study, we evaluated the preclinical characteristics of JAB-2485, a small-molecule inhibitor of AURKA currently in Phase I/IIa clinical trial in the US (NCT05490472). Biochemical studies demonstrated that JAB-2485 is potent and highly selective on AURKA, with subnanomolar IC_{50} and around 1500-fold selectivity over AURKB or AURKC. In addition, JAB-2485 exhibited favorable pharmacokinetic properties featured by low clearance and good bioavailability, strong dose−response relationship, as well as low risk for hematotoxicity and off-target liability. As a single agent, JAB-2485 effectively induced G2/M cell cycle arrest and apoptosis and inhibited the proliferation of small cell lung cancer, triple-negative breast cancer, and neuroblastoma cells. Furthermore, JAB-2485 exhibited robust *in vivo* antitumor activity both as monotherapy and in combination with chemotherapies or the bromodomain inhibitor JAB-8263 in xenograft models of various cancer types. Together, these encouraging preclinical data provide a strong basis for safety and efficacy evaluations of JAB-2485 in the clinical setting.

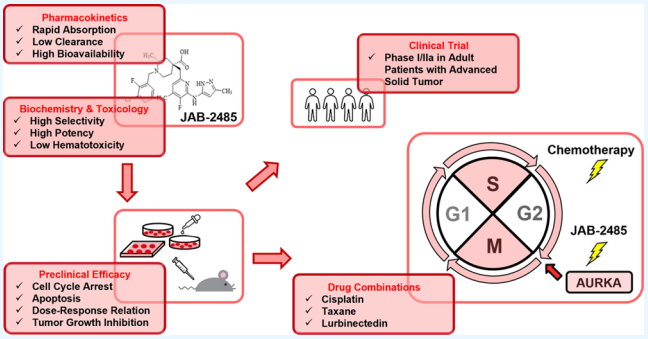

INTRODUCTION

Aurora kinase A (AURKA), along with another Aurora family member of serine/threonine kinase in Aurora kinase B (AURKB), plays essential but distinct roles in the regulation of mitosis and the maintenance of genetic fidelity.[1−4] AURKA activation is subject to exquisite spatiotemporal control under physiological conditions but can be rampant during tumorigenesis.[5,6] Originally named *BTAK* (breast tumor amplified kinase) due to its overexpression in breast tumor cells, *AURKA* has since become a well-recognized oncogene across a wide range of cancer types.[7,8] Indeed, dysregulation of *AURKA*, either amplification or overexpression, is prevalent in cancer and associated with clinical aggressiveness, therapeutic resistance, and poor prognosis.[9−13]

Over the last two decades, independent studies have revealed mechanistic insights into the oncogenic roles of AURKA.[5,14,15] Notably, in small cell lung cancer (SCLC), aberrant activation of AURKA overrides *RB1* loss-primed spindle-assembly checkpoint (SAC) for mitotic exit and tumor cell survival.[16] In breast cancer, AURKA contributes to endocrine resistance through down-regulation of ERα expression and induces epithelial-to-mesenchymal transition to promote distant metastases.[17,18] In *MYCN*-amplified neuroblastoma (NB) cells, AURKA protects N-Myc from FBXW7-mediated proteasomal degradation.[19] Furthermore, in *ARID1A*-deficient colorectal cancer (CRC) and ovarian clear cell carcinoma, tumor cells become addicted to the AURKA-PLK1-CDC25C signaling cascade for survival and proliferation.[20]

Since the disclosure of ZM447439, the first small-molecule Aurora kinase inhibitor, significant progress has been achieved in therapeutic targeting of AURKA in cancer, with over a dozen drug candidates having entered clinical trials and many more being under preclinical development.[5,21] AURKA-selective inhibitors own potential advantages over pan-Aurora kinase inhibitors, as the latter phenocopy AURKB inactivation in polyploidy induction and might jeopardize the therapeutic effects of AURKA inhibition.[22−26] Alisertib (MLN8237, developed by Millennium Pharmaceuticals and Takeda Pharmaceutical Co.), the most extensively studied AURKA inhibitor, has relatively narrow target selectivity on AURKA over AURKB and a generally manageable safety profile with the most frequent toxicity being myelosuppression.[27−29] Despite some encouraging early clinical data, in the only phase 3 trial of

Received: February 22, 2024
Revised: April 3, 2024
Accepted: April 23, 2024
Published: May 3, 2024

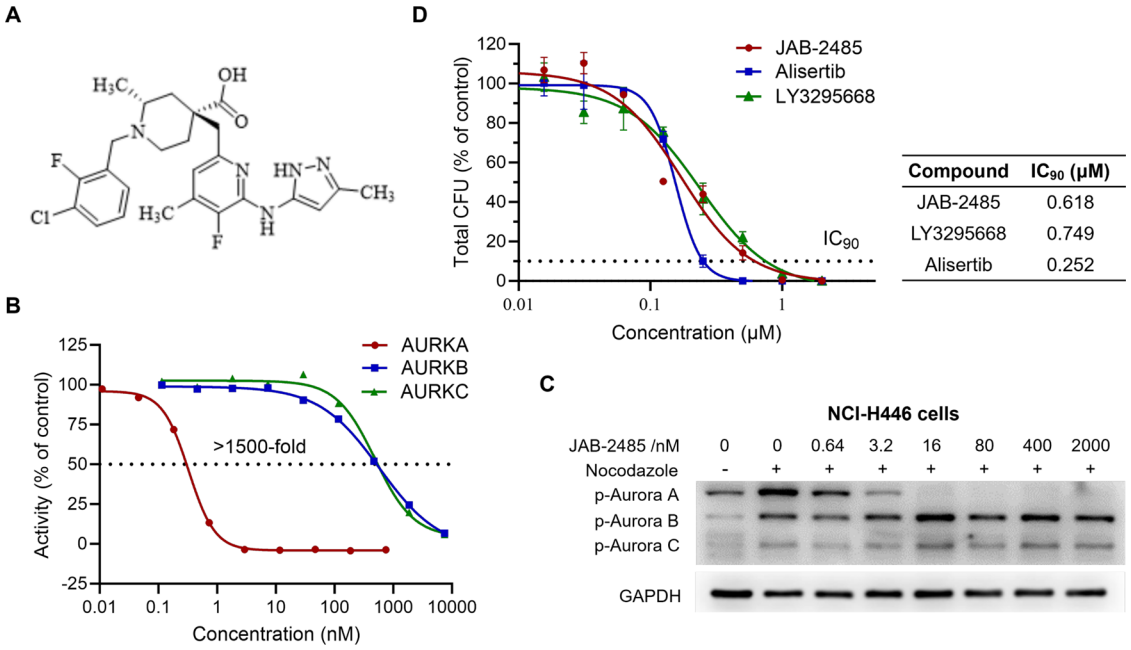

Figure 1. JAB-2485 is a potent, highly selective AURKA inhibitor. (A) Chemical structure of JAB-2485. (B) *In vitro* kinase assay was performed to determine the IC_{50}s of JAB-2485 on Aurora kinase family members. (C) Western blot was performed to examine the phosphorylation of Aurora kinase family members in NCI-H446 cells upon treatment with JAB-2485 at different concentrations. (D) CFU-GM assay was performed to evaluate potential myelosuppression. IC_{90}s of JAB-2485, LY3295668, and alisertib on the colony formation of granulocytes and macrophages were determined.

alisertib as a single agent in relapsed and refractory peripheral T cell lymphoma (R/R-PTCL), it failed to improve the progression-free survival compared to investigator-selected single-agent comparators and was unlikely to produce superior efficacy over currently approved treatment regimens.[30] Several other AURKA-selective inhibitors, including VIC-1911, WJ05129, and LY3295668, are currently in the early stages of clinical trials.[31−37] Overall, the prominent oncogenic roles of AURKA, along with limited beneficial outcomes from AURKA-targeting clinical trials, warrant the development of new AURKA inhibitors with improved potency, safety, and target selectivity as well as the refinement of therapeutic indications and the exploration of drug combination strategies.

We report here the development of JAB-2485, an orally bioavailable, highly selective, small-molecule AURKA inhibitor. JAB-2485 exhibited a promising safety profile and favorable pharmacokinetic properties and efficiently inhibited the growth of a panel of cancer cells by inducing cell cycle arrest and apoptosis. *In vivo* studies on JAB-2485 further demonstrated a strong exposure-response relationship and its robust antitumor activities either as a single agent or in various combination therapies.

RESULTS

JAB-2485 Is a Potent, Highly Selective AURKA Inhibitor. JAB-2485 (Figure 1A) was identified through the drug discovery platform (DDP) integrating medicinal chemistry, biophysical studies, and computational techniques. Briefly, the techniques of structure-based drug design (SBDD) and computer aided design and drafting (CADD) were used to identify the hit compound. The fragment-based drug discovery (FBDD) approach was then applied for hit-to-lead optimization to enhance the compound potency and selectivity. Finally, based on the lead structure, different series of compounds were designed through medicinal chemistry for evaluation of oral bioavailability and *in vivo* efficacy. As a result, JAB-2485 was selected as the top candidate. Enzymatically, JAB-2485 inhibited AURKA with an IC_{50} of 0.327 nM, exhibiting more than 1,500 folds of selectivity over AURKB/AURKC (Figure 1B). In NCI-H446 SCLC cells, treatment of JAB-2485 for 16 h significantly decreased the level of AURKA phosphorylation on Thr288, a marker for AURKA activation,[38] in a dose-dependent manner with an IC_{50} of 2.08 nM (Figure 1C). By contrast, no inhibition of phosphorylation of AURKB and AURKC was observed following drug treatment at concentrations up to 2 μM, indicating that the two Aurora family members were not targeted by JAB-2485.

In terms of hematotoxicity, JAB-2485 significantly differed from alisertib in the inhibition of colony formation of granulocyte-macrophage progenitors, as reflected by compound IC_{90} values (0.618 μM for JAB-2485; 0.252 μM for alisertib), indicating that JAB-2485 is less likely to induce myelosuppression (Figure 1D). In addition, JAB-2485 did not induce a significant off-target effect on the 41 common adverse drug reaction molecules (Table S1). Overall, JAB-2485 exhibits favorable physiochemical properties and safety profiles and targets AURKA with great potency and selectivity.

JAB-2485 Inhibits Cancer Cell Viability by Inducing Cell Cycle Arrest and Apoptosis. At the cellular level, JAB-2485 inhibited the viability of a broad panel of human cancer cell lines. Among the 33 cancer cell lines tested, the potency of JAB-2485 varied, with IC_{50} values ranging from 8.1 nM to greater than 1 μM. Overall, 20 out of 33 (61%) cell lines were sensitive to JAB-2485, as artificially defined by IC_{50} less than 0.1 μM. Among all the lung cancer cell lines tested, the percentage of sensitive cell lines was higher in the *RB1* mutant (4 out of 6; 67%) versus the *RB1*-WT group (2 out of 5; 40%), and in the *MYC/MYCN*-amplified (5 out of 7; 71%) versus the non-amplified group (1 out of 4; 25%) (Table 1). Additionally, all four (100%) NB cell lines were highly sensitive to JAB-2485 with

https://doi.org/10.1021/acsomega.4c01752
ACS Omega 2024, 9, 21416−21425

Table 1. IC_{50}s of JAB-2485 on Lung Cancer Cell Lines with *RB1* Mutations or *MYC* Amplification

cell line	cancer type	RB1	MYC	IC_{50} (nM)
NCI-H69	SCLC	nonsense	MYCN amp	29.7
NCI-H2171	SCLC	nonsense	MYC amp	46.1
NCI-H446	SCLC	splice site	MYC amp	51.8
NCI-H1975	NSCLC	WT	MYC amp	54.4
NCI-H526	SCLC	nonsense	MYCN amp	55.6
Calu-6	NSCLC	WT	WT	64.9
SW1271	SCLC	WT	WT	225
NCI-H82	SCLC	splice site	MYC amp	249
NCI-H1650	NSCLC	WT	WT	365
NCI-H209	SCLC	missense	WT	406
DMS53	SCLC	splice site	MYC amp	982

an average IC_{50} of 17.3 nM; and 6 out of 8 (75%) triple-negative breast cancer (TNBC) cell lines (all with *MYC* amplification), 2 out of 5 (40%) ovarian cancer cell lines, and 2 out of 5 (40%) colon cancer cell lines were categorized as drug sensitive (Table S2). The average IC_{50} values were 50.4 and 68.0 nM, respectively, for the sensitive breast and lung cancer cell lines. Collectively, we demonstrated the *in vitro* potency and efficacy of JAB-2485, particularly in NB, TNBC, and *RB1*-null and/or *MYC/MYCN*-amplified lung cancer cells.

As AURKA plays an indispensable role in mitotic progression, its inhibition by JAB-2485 is expected to induce cell cycle arrest. Indeed, in NCI-H446 cells, treatment of JAB-2485 for 24 h significantly increased the G2/M phase DNA content in a dose-dependent manner, indicative of cell stagnation (Figure 2A). Furthermore, we found a dose-dependent significant increase of Caspase 3/7 activity in NCI-H446 cells with treatment of JAB-2485 at concentrations as low as 0.12 μM compared to the control group, indicating that JAB-2485 can efficiently induce apoptosis of cancer cells (Figure 2B).

JAB-2485 Exhibits Favorable PK Properties and Strong PK/PD Relationship. JAB-2485 was rapidly absorbed after oral administration with T_{max} of 1.17 and 0.417 h in rats and dogs, respectively. In addition, JAB-2485 showed low clearance, with clearance rates of 0.729 and 3.96 mL/min in rats and dogs, respectively. The V_{ss} was determined as 0.278 and 0.559 L/kg, and bioavailability as 81.1 and 78.8% in rats and dogs, respectively (Table 2). Overall, JAB-2485 had favorable pharmacokinetic profiles.

Table 2. Pharmacokinetics of JAB-2485 at a Single Dose in Different Species[a]

	rat		dog	
dose (mg/kg)	0.5	0.5	1	1
rte. of admin.	IV[b]	PO[c]	IV[b]	PO[c]
CL (mL/min/kg)	0.729		3.96	
V_{ss} (L/kg)	0.278		0.559	
T_{max} (h)		1.17		0.417
$T_{1/2}$ (h)	5.1	4.36	3.56	4.8
F%		81.1		78.8

[a]IV: intravenous injection; PO: oral administration. [b]10% DMSO, 20% PEG400, 70% Saline. [c]0.5% CMC-Na in water.

The NCI-H446 xenograft model was used to study the relationship between the biological activity of JAB-2485 and its exposure. Phosphorylation of AURKA on Thr288 and phosphorylation of histone H3 on Ser10 in tumor tissues, indicative of AURKA activity and mitotic arrest, respectively, were evaluated as potential PD markers.[38,39] Corresponding concentrations of JAB-2485 in both plasma and tumor tissues were measured by LC−MS/MS for correlation analyses. Upon single oral administration of JAB-2485 at 10 mg/kg, AURKA phosphorylation was decreased in a time-dependent manner, with around 80% of inhibition reached within the first hour and maintained for up to 12 h (Figure 3A). Under the same treatment conditions, histone H3 phosphorylation was increased starting within the first hour and peaked 12 h after administration (Figure 3B). JAB-2485 showed a rapid absorption and clearance rate, as the concentration reached a peak in plasma (14700 ng/mL) within 0.25 h and decreased to near baseline after 24 h. In tumor tissues, the concentration peaked at 1507 ng/g within 1 h and fell below 100 ng/g after 12 h (Figure 3A,B). To determine whether AURKA signaling inhibition was dose-dependent, JAB-2485 was orally administered as a single dose of 2.5, 5, 10, and 20 mg/kg. Indeed, AURKA phosphorylation decreased within 1 h by 50.1, 73.0, 89.4, and 92.5%, respectively, along with a dose-dependent increase of drug exposure in plasma and tissue (Figure 3C). Conclusively, JAB-2485 produced potent and prolonged AURKA signaling inhibition and mitotic arrest *in vivo* in a dose-dependent manner.

JAB-2485 Suppresses Tumor Growth as a Monotherapy. Based on the prominent *in vitro* efficacy of JAB-2485, we

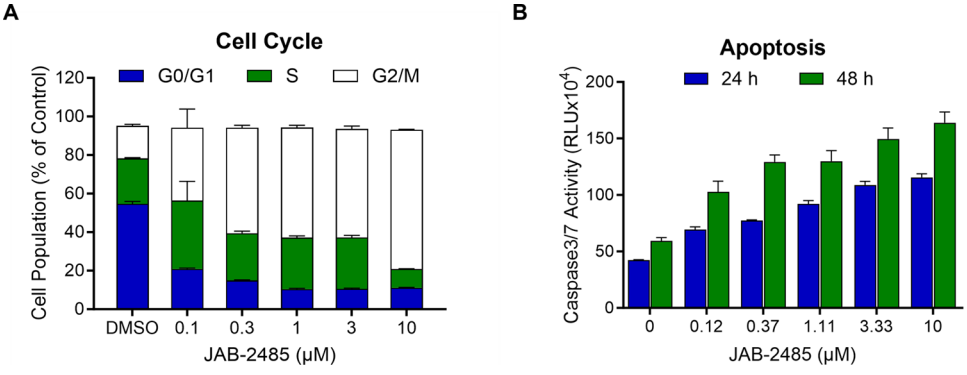

Figure 2. JAB-2485 inhibits cancer cell viability by inducing cell arrest and apoptosis. (A) NCI-H446 cells were treated with JAB-2485 at different concentrations for 24 h. Flow cytometry was performed to determine the percentage of cell populations at different stages of the cell cycle. (B) NCI-H446 cells were treated with JAB-2485 at different concentrations for 24 or 48 h. Caspase 3/7 activities were determined as measures of luminous intensities.

https://doi.org/10.1021/acsomega.4c01752
ACS Omega 2024, 9, 21416−21425

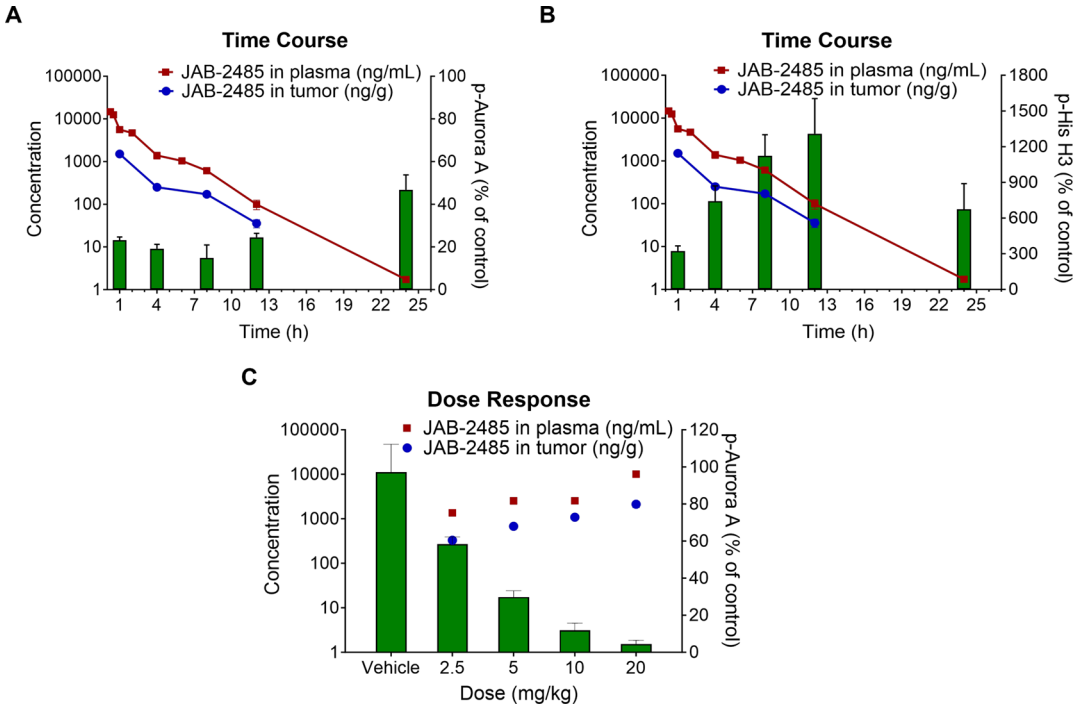

Figure 3. JAB-2485 exhibits a strong PK/PD relationship in the NCI-H446 xenograft model. (A and B) JAB-2485 was orally administered at 10 mg/kg, and the time course of JAB-2485 concentrations in plasma and tumor tissues as well as AURKA phosphorylation (A) and histone H3 phosphorylation (B) in tumor tissues (both as a percentage of the vehicle control) was determined. Three mice per time point. (C) JAB-2485 was orally administered at indicated doses, and the concentrations of JAB-2485 in plasma and tumor tissues, as well as the phosphorylation of AURKA in tumor tissues (as a percentage of the vehicle control), at 1 h after administration were determined. Three mice per dose.

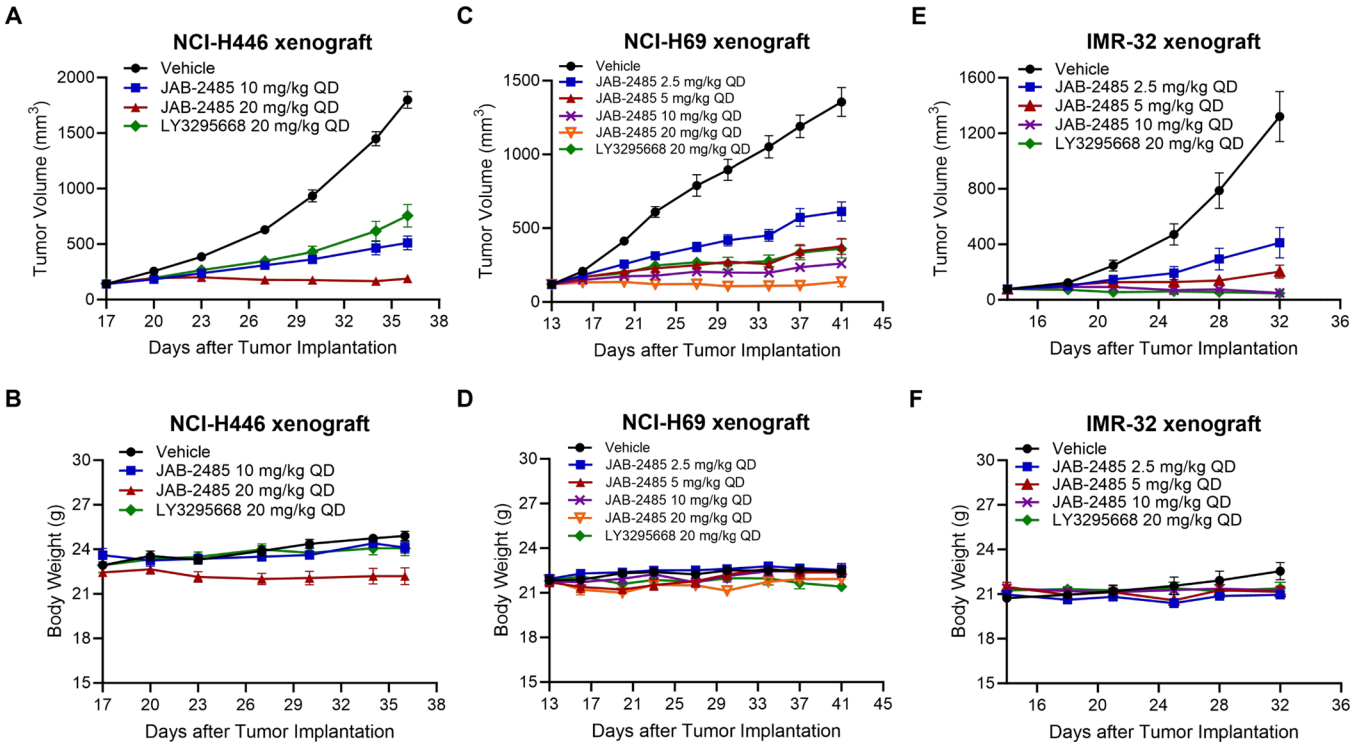

Figure 4. JAB-2485 suppresses tumor growth as a monotherapy. In NCI-H446, NCI-H69, and IMR-32 xenografts, JAB-2485 or LY3295668 was orally administered at indicated doses, and tumor volumes (A–E) and body weights (B–F) were measured. Nine mice per treatment group.

used SCLC and NB xenograft models to evaluate the *in vivo* antitumor activity of JAB-2485 monotherapy as well as its dosing regimen. In the NCI-H446 xenograft model, treatment with JAB-2485 at 10 and 20 mg/kg QD led to 78 and 97% tumor growth inhibition (TGI), respectively ($p < 0.001$, compared to vehicle control), which were superior to the TGI of 63% by LY3295668, another AURKA-selective inhibitor, at 20 mg/kg QD (Figure 4A). No significant toxicity or body weight loss was

https://doi.org/10.1021/acsomega.4c01752
ACS Omega 2024, 9, 21416−21425

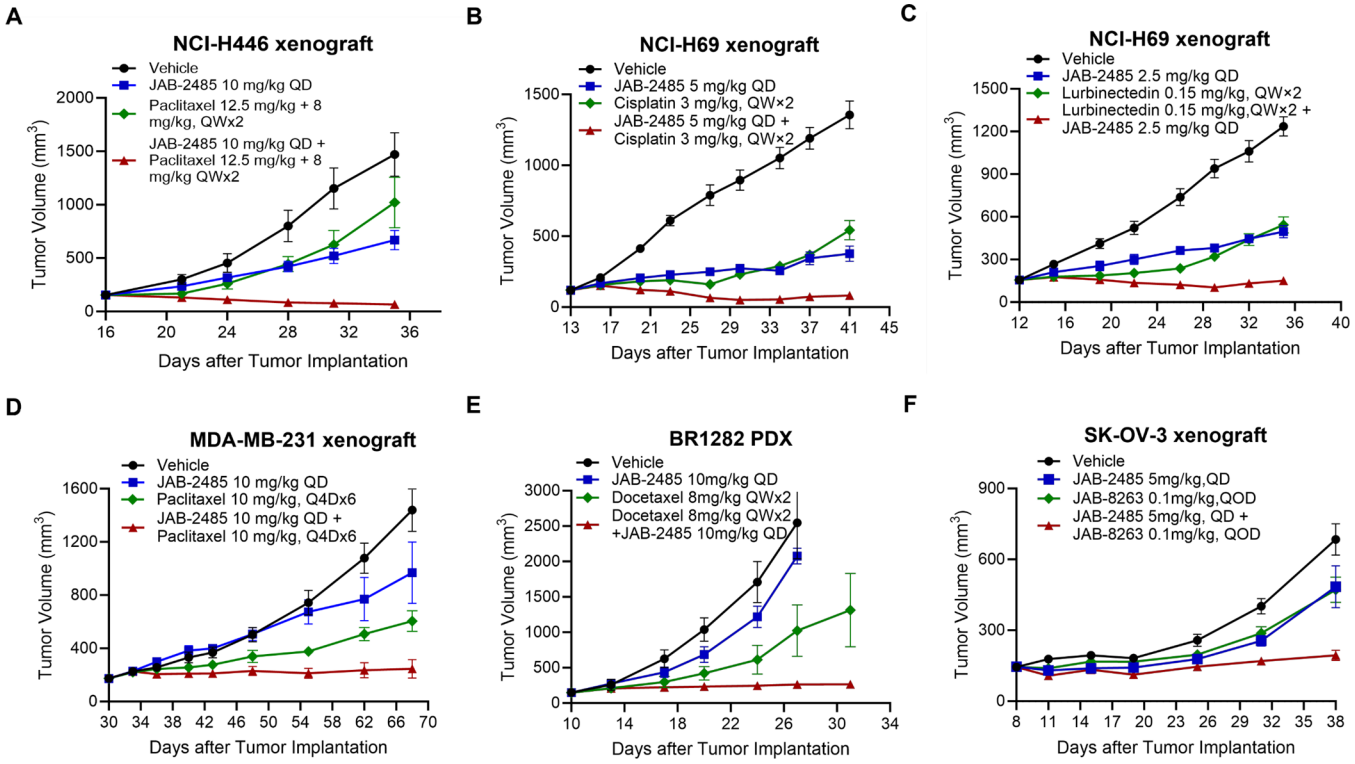

Figure 5. JAB-2485 enhances antitumor activities in combination therapies. The antitumor activities of JAB-2485 in combination with paclitaxel in the NCI-H446 lung cancer xenograft (A); with cisplatin in the NCI-H69 lung cancer xenograft (B); with lurbinectedin in the NCI-H69 lung cancer xenograft (C); with paclitaxel in the MDA-MB-231 breast cancer xenograft (D); with docetaxel in the BR1282 breast cancer xenograft (E); and with JAB-8263 in the SK-OV-3 ovarian cancer xenograft (F) were evaluated. Tumor volumes were measured with 9 mice per treatment group (A–D and F) or 3 mice per treatment group (E).

observed during the treatment period for all groups, indicating that JAB-2485 was generally well-tolerated (Figure 4B). In the NCI-H69 SCLC xenograft model, treatment with JAB-2485 at 2.5, 5, 10, and 20 mg/kg QD significantly inhibited tumor growth in a dose-dependent manner with TGIs of 60, 79, 89, and 99%, respectively ($p < 0.001$, compared to vehicle control). In comparison, TGI of 79% was achieved by treatment with LY3295668 at 20 mg/kg QD (Figure 4C). Consistently, there was an insignificant body weight change in all treatment groups, indicating good tolerability of JAB-2485 (Figure 4D). Furthermore, in the IMR-32 NB xenograft model, TGIs of 73, 90, and 102% were achieved for the 2.5, 5, and 10 mg/kg QD groups ($p = 0.008$, 0.002, and 0.001, respectively, compared to vehicle control) without significant body weight loss observed (Figure 4E,F). Treatment of LY3295668 at 20 mg/kg QD led to TGI comparable to that of the JAB-2485 10 mg/kg QD group. In addition, the AUC_{0-24h} of JAB-2485 plasma exposure in the three treatment groups were 5,703, 12,044, and 22,748 ng h/mL, respectively, corresponding to the dose increase (Table S3). Overall, in the xenograft models tested, JAB-2485 exhibited strong antitumor activity and good tolerability as a single agent.

JAB-2485 Is a Promising Drug Candidate in Combination Therapies. In previous studies, AURKA inhibitors have been demonstrated to enhance the efficacy and/or overcome the resistance of diverse chemotherapies and targeted therapies.[40] Considering the promising early efficacy and safety data, we further explored the application of JAB-2485 through the rational design of combination strategies targeting different indications. As AURKA inhibitors induce microtubule destabilization during mitosis, they may synergize with cell cycle inhibitors in targeting tumor cells. While JAB-2485 exhibited strong antitumor activities as a single agent in SCLC xenografts, we investigated whether its combination with microtubule inhibitors or other categories of cell cycle inhibitors could further enhance the efficacy. Indeed, in the NCI-H446 xenograft model, combined treatment with JAB-2485 at 10 mg/kg QD and paclitaxel at 12.5 mg/kg on Day 16 and 8 mg/kg on Day 24 led to impressive 107% TGI ($p < 0.001$), superior to both single drugs at the same dosage (JAB-2485 with 61% TGI, $p = 0.001$; paclitaxel with 34% TGI, $p = 0.054$) (Figure 5A). In the NCI-H69 xenograft model, TGIs of 79, 66, and 103% (all $p < 0.001$) were achieved by treatment with JAB-2485 at 5 mg/kg QD, cisplatin at 3 mg/kg QW × 2, and the two-drug combination with same dosage, respectively (Figure 5B). In the same model, TGIs of 69, 64, and 101% (all $p < 0.001$) were achieved by treatment with JAB-2485 at 2.5 mg/kg QD, lurbinectedin at 0.15 mg/kg QW × 2, and the two-drug combination with same dosage, respectively (Figure 5C).

In addition to SCLC, the *in vivo* efficacy of JAB-2485 was evaluated in TNBC models. In the MDA-MB-231 xenograft model, JAB-2485 at 10 mg/kg QD, paclitaxel at 10 mg/kg Q4D × 6, and the two-drug combination with same dosage led to TGIs of 37% ($p = 0.075$), 66% ($p = 0.004$), and 94% ($p < 0.0001$), respectively (Figure 5D). Consistently, in the BR1282 TNBC PDX model, JAB-2485 at 10 mg/kg QD, docetaxel at 8 mg/kg QW × 2, and the two-drug combination with same dosage led to TGIs of 20, 63, and 95%, respectively (Figure 5E). These results indicated that JAB-2485 in combination with taxanes significantly enhanced the antitumor activity of either single agent in TNBC xenografts.

Furthermore, recent studies have demonstrated the synthetic lethality between AURKA inhibition and *ARID1A* loss.[20] As

https://doi.org/10.1021/acsomega.4c01752
ACS Omega 2024, 9, 21416−21425

ARID1A negatively regulates the transcription of *AURKA*, its deficiency can lead to aberrant upregulation of AURKA and downstream CDC25C signaling for uncontrolled mitosis, rendering tumor cells addictive to AURKA activation. Intriguingly, *ARID1A* loss also elicits dissociation of histone deacetylase 1 and resultant increase of histone H4 lysine acetylation at the gene enhancer, facilitating the binding of BET protein BRD4 for transcriptional activation of oncogenes.[41−44] In this regard, coinhibition of AURKA and BRD4 represents a tentative strategy targeting *ARID1A*-deficient tumor. In an *ARID1A*-deficient SK-OV-3 ovarian cancer xenograft model, treatment of JAB-2485 at 5 mg/kg QD and JAB-8263, a potent BET protein inhibitor developed by us,[45,46] at 0.1 mg/kg QOD led to TGIs of 37 and 40%, respectively. A significantly increased TGI of 91% was achieved when the mice were treated with both drugs at the same dosage (Figure 5F). For all the above-mentioned xenograft models, no significant change in body weight was observed throughout the treatment period (Figure S1). In summary, JAB-2485 has shown great potential in synergizing with diverse cancer therapeutics *in vivo*.

DISCUSSION

In the current study, we demonstrated several unique characteristics of JAB-2485, which together may distinguish it from other AURKA inhibitors under development. First, JAB-2485 exhibits around 1,500-fold selectivity on AURKA versus AURKB in the enzymatic assay and over 2000-fold preferential AURKA-targeting in the cell-based assay, rendering it by far one of the most selective AURKA inhibitors reported. Furthermore, JAB-2485 is very potent, with IC_{50} in the subnanomolar range based on the *in vitro* kinase assay of AURKA. With its high selectivity and potency on AURKA, JAB-2485 can not only induce profound and sustained mitotic arrest but also circumvent potential DNA endoreduplication and subsequent polyploidy, a common phenotype produced by pan-Aurora inhibitors due to targeting of AURKB, particularly at high plasma concentrations.[22−26] In this regard, JAB-2485 seems less likely to induce chromosome instability and drug resistance, which can be attributed to polyploidy.

Second, JAB-2485 exhibits a favorable safety profile based on GLP safety pharmacology studies. For the cardiovascular system, the *in vitro* IC_{50} value for the inhibitory effect of JAB-2485 on hERG potassium current was 26.7 μM using the manual patch-clamp technique. Consistently, no drug-induced prolongation of the QT interval on the electrocardiogram was observed in conscious Beagle dogs. Other electrocardiogram parameters, heart rate, and blood pressure were within the normal range following JAB-2485 administration. Meanwhile, key parameters of the respiratory system, such as respiratory rate, tidal volume, and minute volume as well as central nervous system-related behavioral functions, were assessed, with no adverse events of these systems identified following JAB-2485 treatment. In addition, at concentrations active against tumor cells, JAB-2485 elicited minimal toxicity to bone marrow cells and therefore is much less likely to induce clinical myelosuppression, which is by contrast the most common side effect reported on alisertib.[27−29] The high selectivity of JAB-2485 may in part contribute to its favorable safety profile compared to those of more promiscuous Aurora inhibitors.

Third, our studies on PK/PD relationships using the NCI-H446 xenograft model demonstrated that the concentration of JAB-2485 rapidly reached the peak in both plasma and tumor tissues following single oral administration. While the drug concentration was low at 12 h after treatment, it induced strong and prolonged AURKA signaling inhibition and cell cycle arrest, as evidenced, respectively, by a decrease of AURKA phosphorylation and an increase of histone H3 phosphorylation in a dose-dependent manner. These findings support the exploration and validation of the above-mentioned PD markers in the clinical settings and provide guidance on the dosing regimen.

Finally, our studies highlighted the therapeutic potential of JAB-2485 in various indications. Amplifications of the MYC oncogene family members are common driver events in SCLC, TNBC, and NB.[47−49] While the first MYC inhibitor, OMO-103, has recently entered clinical trial,[50] the drug's mechanism of action as well as its on-target engagement remains controversial. At present, direct inhibition of MYC remains a challenge due to its complex protein structure. Targeting AURKA to induce SCF^{FBXW7}-mediated MYC proteolysis represents a promising strategy to address the unmet clinical need.[19] Furthermore, functional loss of RB1 is a hallmark of cancer and prevalent in SCLC.[51,52] Previous studies showed that loss of *RB1* and *TP53* contributes to aggressive phenotypes of MYC-driven SCLC, and tumor cells rely on aberrantly activated AURKA to override *RB1* loss-induced SAC for survival.[16,47] In line with previous studies, we demonstrated superior antitumor efficacy of JAB-2485 in *RB1*-deficient and/or MYC family member-amplified tumor models with overall good tolerability. Notably, compared to LY3295668, which also exhibits minimal myelosuppression, JAB-2485 was more potent in the xenograft models tested. It remains to be seen whether these promising features can be translated into clinical outcomes, as a Phase I/IIa clinical trial evaluating JAB-2485 as a monotherapy in adult patients with advanced solid tumors is ongoing in the US (NCT05490472).[53]

In the evaluation of combination therapies, JAB-2485 dramatically enhanced the efficacy of chemotherapeutic drugs in diverse xenograft models. Notably, JAB-2485 in combination with lurbinectedin induced tumor regression compared to 64% of TGI by lurbinectedin alone in the SCLC NCI-H69 xenograft model. Lurbinectedin as a second-line treatment for patients with SCLC has achieved an overall response rate of 35.2% in a single-arm, open-label, phase 2 basket trial.[54] Our study indicated the JAB-2485-lurbinectedin combination as a potential new treatment strategy, especially for those with limited options in the event of a relapse. Furthermore, in a randomized Phase II trial, alisertib combined with paclitaxel improved progression-free survival of patients with relapsed or refractory SCLC compared to treatment of paclitaxel alone.[55] We envision a forthcoming clinical trial of JAB-2485 in combination with chemotherapeutic drugs firmly supported by our preclinical data. Finally, JAB-2485 potentially synergized with JAB-8263, a clinical stage BET protein inhibitor,[45,46] in an *ARID1A*-deficient ovarian cancer xenograft model. The results were in line with several recent studies showing the promise of AURKA/BET coinhibition in different indications. Notably, the AURKA/BET inhibitor duo was identified as one of the most potent drug combinations targeting glioblastoma in a high-throughput screening, which was further validated in spheroid models and syngeneic orthotopic mouse models.[56] In addition, alisertib in combination with the BET inhibitor JQ1 showed profound efficacy in *MYCN*-amplified, *TP53*-wild-type NB mouse models.[57] Furthermore, BET inhibitors were demonstrated to block the growth of TNBC through suppression of Aurora kinases.[58] Our results along with these findings have provided the basis for potential testing of JAB-2485 in

https://doi.org/10.1021/acsomega.4c01752
ACS Omega 2024, 9, 21416−21425

combination with JAB-8263 in the clinical setting. Further exploration of combination strategies is warranted, particularly with rationalized chemotherapies and targeted therapies on pertinent indications refined by robust biomarkers. Overall, we established JAB-2485 as a welcome addition to the treatment options for cancer patients.

MATERIALS AND METHODS

Cell Lines, Culture Media, and Antibodies. SCLC cell lines NCI-H69, NCI-H2171, NCI-H446, NCI-H525, NCI-H82, NCI-H209, SW1271, and DM553, non-small cell lung cancer (NSCLC) cell lines NCI-H1975, NCI-H1650, and Calu-6, TNBC cell lines Hs578T, BT20, BT549, HCC1806, HCC1143, HCC1395, HCC70, and DU4475, epithelial ovarian cancer (EOC) cell lines CoC1, A2780, EFO-27, SK-OV-3, and SW756, NB cell lines SH-SY5Y, IMR-32, Daoy, and SK-N-SH, CRC cell lines Km12L4, SW48, SW948, SNU-81, and HCT-15 were purchased from The American Type Culture Collection (ATCC, Manassas, VA, United States) and cultured using ATCC-recommended media. Antibody against phospho-Aurora A (Thr288)/Aurora B (Thr232)/Aurora C (Thr198) was purchased from Cell Signaling Technology (Danvers, MA, Catalog #2914).

Test Compounds. JAB-2485, JAB-8263, and LY3295668 were synthesized by Jacobio Pharmaceuticals; alisertib was purchased from MedChemExpress (Monmouth Junction, NJ, United States); and paclitaxel, docetaxel, cisplatin, and lurbinectedin were purchased from Beijing Ouhe Technology Co. Ltd. (Beijing, China).

Enzymatic Assays. The Aurora family kinase assay was performed by Pharmaron Beijing Co., Ltd. (Beijing, China). JAB-2485 was incubated at concentrations of 0.00382−1000 nM in reaction buffer containing AURKA, AURKB, and AURKC for 30 min before assay termination. The assay plates were subjected to the EZ reader and subsequent analyses. The percentage of remaining enzyme activity was calculated using the conversion ratio (CR) following the equation: % Remaining Activity = 100% − 100% × (CR_{HC} − CR_{Sample})/(CR_{HC} − CR_{LC}). CR_{HC}: DMSO; CR_{Sample}: sample data; CR_{LC}: no enzyme. XLFit (eq 201) was used to calculate IC_{50}: $y = A + (B - A)/(1+(x/C)\ ^{\wedge}D))$. A: Bottom; B: Top; C: IC_{50}; D: Hill slope.

Immunoblotting. NCI-H446 cells were pretreated with nocodazole (100 ng/mL) for 3 h before incubation of JAB-2485 at indicated concentrations for 2 h. Total protein was extracted from cells using RIPA buffer added with Halt Protease Inhibitor Cocktail, resolved by SDS-PAGE under reducing conditions, and transferred onto PVDF membranes. The expression of phosphorylated AURKA/AURKB/AURKC was detected by Amersham Imager 600, and the intensity of bands was analyzed by the GE Gel Analysis System (Chicago, IL, United States). The absolute IC_{50} on AURKA phosphorylation was calculated based on the intensity of bands and according to the dose−response curve generated by GraphPad Prism 8.0 (GraphPad Software, Boston, MA, United States).

Colony-Forming Unit-Granulocyte-Macrophage (CFU-GM) Assay. The CFU-GM assay was performed by STEMCELL Technologies (Cambridge, MA, United States). In brief, frozen human bone marrow mononuclear cells were added to aliquots of MethoCult GF H84534 containing a test or controlled compound and mixed well. The cells were then plated into 3 replicate wells of a 6-well SmartDish and cultured at 37 °C and 5% CO_2 for 13−15 days. The total number of CFU-GM colonies was evaluated by trained personnel and enumerated based on morphology. The resulting colony numbers from test and control compound-treated cultures were compared to solvent control cultures to determine percent of control growth, and dose response curves were generated and IC_{90} values were derived.

Cell Proliferation Assay. The study was performed by Crown Bioscience (Beijing, China). Briefly, tumor cells were plated in 96-well flat clear bottom black polystyrene TC-treated microplates (Corning) with a final cell density of 4×10^3 cells/well and allowed to attach overnight. Drugs at various concentrations were dispensed in each well. Five days after treatment, cell viability was measured by the CellTiter-Glo Luminescent Cell Viability Assay (Promega) using EnVision Multi Label Reader 2104-0010A (PerkinElmer).

Flow Cytometry. NCI-H446 cells were seeded in 6-well plates at a density of 4×10^5 cells/well and pretreated with JAB-2485 at the indicated concentrations for 24 h. Cells were then harvested and fixed using FxCycle PI/RNase Staining Solution (Invitrogen, Catalog #F10797). The cell cycle was measured using a MACSOuant Analyzer (Miltenyi Biotec, Gaithersburg, MD, United States). Cell cycle analysis was performed based on the distribution of DNA content using Flow Jo software (Ashland, OR, United States).

Caspase 3/7 Assay. NCI-H446 cells were cultured overnight in a 96-well plate (1×10^4 cells/well) before treatment with JAB-2485 at the indicated concentrations for 24 and 48 h. Caspase 3/7 reagents were added to each well and incubated at room temperature for 1 h. The luminescence was measured by a Spark multimode microplate reader (Tecan, Männedorf, Switzerland).

***In Vivo* PK and PK/PD Analyses.** For the PK study, blood samples were obtained at 0, 0.033, 0.083, 0.25, 0.5, 1, 2, 4, 6, 8, 12, and 24 h after dosing with JAB-2485 from 3 animals/sex/time point in SD rat and beagle dog. Plasma samples were prepared and analyzed for JAB-2485 concentrations by LC−MS/MS. All PK parameters were calculated using noncompartment models of WinNonlin 6.3 or above (Pharsight, Mountain View, CA, United States).

For the time-dependent PK/PD study, each female BALB/c nude mouse bearing NCI-H446 tumors was administrated orally with a single dose of JAB-2485 at 10 mg/kg. The groups of mice were sacrificed, and then blood and tumor tissues were collected for PK and PD analysis at the indicated time points. For the dose-dependent PK/PD study, each female BALB/c nude mouse bearing NCI-H446 tumors was administrated orally with a single dose of JAB-2485 at 2.5, 5, 10, and 20 mg/kg, and plasma and tumor samples were collected for PK and PD analysis at 1 h after drug administration. Tumor tissue was analyzed by Western blot to determine phospho-AURKA (p-Aur A) and phospho-Histone H3 (p-HisH3) levels, and the plasma/tumor drug concentration of JAB-2485 was quantified using the LC−MS/MS method. PK/PD correlation was established by comparing p-Aur A and p-HisH3 levels with drug concentration at each time point.

***In Vivo* Efficacy Studies.** The protocol, procedures, and any amendments involved in the care and use of animals in the BR1282 TNBC PDX model study were reviewed and approved by the Institutional Animal Care and Use Committee (IACUC) of Crown Bioscience (Beijing, China). All other animal experiments were conducted under procedures approved by the IACUC at Jacobio Pharmaceuticals.

https://doi.org/10.1021/acsomega.4c01752
ACS Omega 2024, 9, 21416−21425

Mice were maintained at a maximum of 5 mice per cage with 12 light/dark cycles. Each mouse was inoculated subcutaneously in the right flank region with tumor cells for tumor development. Mice were monitored daily, and caliper measurements were performed once the tumors became visible. Tumor volume was calculated by measuring two perpendicular diameters using the formula: $(L \times W\ 2)/2$ in which L and W refer to tumor length and width, respectively. When the average tumor volume reached 100−200 mm^3, mice were grouped randomly and treated with compounds. Tumor volume and body weight were measured twice a week during treatment. TGI rates were calculated as follows: TGI% = $(1 - (V_t - V_{t0})/(V_c - V_{c0}))$ *100%, wherein V_c and V_t are the mean tumor volumes of control and treated groups at the end of the experiments, respectively; and V_{c0} and V_{t0} are the mean tumor volumes of control and treated groups at the start of the experiments, respectively.

Statistical Analyses. Statistical summaries included the mean and the standard error of the mean (SEM). Statistical analysis of difference in tumor volume or tumor weight among the groups was performed using one-way ANOVA, followed by individual comparisons using the LSD test (equal variance assumed) or the Games-Howell posthoc test (equal variance not assumed). All data was analyzed using SPSS 22.0 software. $P < 0.05$ was defined as statistically significant. *, $P < 0.05$; **, $P < 0.01$; and ***, $P < 0.001$.

■ ASSOCIATED CONTENT

Supporting Information

The Supporting Information is available free of charge at https://pubs.acs.org/doi/10.1021/acsomega.4c01752.

Preclinical safety pharmacology on off-target activity of JAB-2485; IC_{50}s of JAB-2485 on breast cancer, ovarian cancer, neuroblastoma, and colorectal cell lines; pharmacokinetics of JAB-2485 at daily dose in plasma of the IMR-32 xenograft model; and the body weights of animals related to Figure 5 (PDF)

■ AUTHOR INFORMATION

Corresponding Author

Yanping Wang − *Jacobio Pharmaceuticals Co., Ltd., Beijing 100176, China;* orcid.org/0009-0009-9498-2124; Email: yanping.wang@jacobiopharma.com

Authors

Guiqun Yang − *Jacobio Pharmaceuticals Co., Ltd., Beijing 100176, China*

Yiwei Lin − *Jacobio Pharmaceuticals Co., Ltd., Beijing 100176, China*

Xin Sun − *Jacobio Pharmaceuticals Co., Ltd., Beijing 100176, China*

Dai Cheng − *Jacobio Pharmaceuticals Co., Ltd., Beijing 100176, China*

Haijun Li − *Jacobio Pharmaceuticals Co., Ltd., Beijing 100176, China*

Shizong Hu − *Jacobio Pharmaceuticals Co., Ltd., Beijing 100176, China*

Mingming Chen − *Jacobio Pharmaceuticals Co., Ltd., Beijing 100176, China*

Yinxiang Wang − *Jacobio Pharmaceuticals Co., Ltd., Beijing 100176, China*

Complete contact information is available at: https://pubs.acs.org/10.1021/acsomega.4c01752

Author Contributions

Conceptualization and supervision: Y.W. and Y.W.; methodology, data acquisition, analysis, and interpretation: G.Y., Y.L., X.S., D.C., H.L., S.H., and M.C.; original draft preparation and editing: Y.L. and X.S. G.Y. and Y.L. contributed equally to this work.

Notes

The authors declare no competing financial interest.

■ ACKNOWLEDGMENTS

We thank Andrea Wang-Gillam at Jacobio for advice on experimental design, data interpretation, and comments on the manuscript. We also thank STEMCELL Technologies for the development and performance of the CFU-GM assay and Crown Bioscience for performance of the cell proliferation assay and *in vivo* efficacy studies.

■ REFERENCES

(1) Carmena, M.; Earnshaw, W. C. The cellular geography of aurora kinases. *Nat. Rev. Mol. Cell Biol.* **2003**, *4*, 842−854.

(2) Marumoto, T.; Zhang, D.; Saya, H. Aurora-A - a guardian of poles. *Nat. Rev. Cancer* **2005**, *5*, 42−50.

(3) Glover, D. M.; Leibowitz, M. H.; McLean, D. A.; Parry, H. Mutations in aurora prevent centrosome separation leading to the formation of monopolar spindles. *Cell* **1995**, *81*, 95−105.

(4) Bischoff, J. R.; Plowman, G. D. The Aurora/Ipl1p kinase family: regulators of chromosome segregation and cytokinesis. *Trends Cell Biol.* **1999**, *9*, 454−459.

(5) Du, R.; Huang, C.; Liu, K.; Li, X.; Dong, Z. Targeting AURKA in Cancer: molecular mechanisms and opportunities for Cancer therapy. *Mol. Cancer* **2021**, *20*, 15.

(6) Cacioppo, R.; Lindon, C. Regulating the regulator: a survey of mechanisms from transcription to translation controlling expression of mammalian cell cycle kinase Aurora A. *Open Biol.* **2022**, *12*, No. 220134.

(7) Sen, S.; Zhou, H.; White, R. A. A putative serine/threonine kinase encoding gene BTAK on chromosome 20q13 is amplified and overexpressed in human breast cancer cell lines. *Oncogene* **1997**, *14*, 2195−2200.

(8) Zhou, H.; Kuang, J.; Zhong, L.; Kuo, W. L.; Gray, J. W.; Sahin, A.; Brinkley, B. R.; Sen, S. Tumour amplified kinase STK15/BTAK induces centrosome amplification, aneuploidy and transformation. *Nat. Genet.* **1998**, *20*, 189−193.

(9) Zheng, D.; Li, J.; Yan, H.; Zhang, G.; Li, W.; Chu, E.; Wei, N. Emerging roles of Aurora-A kinase in cancer therapy resistance. *Acta Pharm. Sin B* **2023**, *13*, 2826−2843.

(10) Zhang, J.; Li, B.; Yang, Q.; Zhang, P.; Wang, H. Prognostic value of Aurora kinase A (AURKA) expression among solid tumor patients: a systematic review and meta-analysis. *Jpn. J. Clin Oncol* **2015**, *45*, 629−636.

(11) Jeng, Y. M.; Peng, S. Y.; Lin, C. Y.; Hsu, H. C. Overexpression and amplification of Aurora-A in hepatocellular carcinoma. *Clin. Cancer Res.* **2004**, *10*, 2065−2071.

(12) Tong, T.; Zhong, Y.; Kong, J.; Dong, L.; Song, Y.; Fu, M.; Liu, Z.; Wang, M.; Guo, L.; Lu, S.; et al. Overexpression of Aurora-A contributes to malignant development of human esophageal squamous cell carcinoma. *Clin. Cancer Res.* **2004**, *10*, 7304−7310.

(13) Reiter, R.; Gais, P.; Jutting, U.; Steuer-Vogt, M. K.; Pickhard, A.; Bink, K.; Rauser, S.; Lassmann, S.; Hofler, H.; Werner, M.; Walch, A. Aurora kinase A messenger RNA overexpression is correlated with tumor progression and shortened survival in head and neck squamous cell carcinoma. *Clin. Cancer Res.* **2006**, *12*, 5136−5141.

(14) Katayama, H.; Brinkley, W. R.; Sen, S. The Aurora kinases: role in cell transformation and tumorigenesis. *Cancer Metastasis Rev.* **2003**, *22*, 451−464.

(15) Hilton, J. F.; Shapiro, G. I. Aurora kinase inhibition as an anticancer strategy. *J. Clin Oncol* **2014**, *32*, 57−59.
(16) Gong, X.; Du, J.; Parsons, S. H.; Merzoug, F. F.; Webster, Y.; Iversen, P. W.; Chio, L. C.; Van Horn, R. D.; Lin, X.; Blosser, W.; et al. Aurora A Kinase Inhibition Is Synthetic Lethal with Loss of the RB1 Tumor Suppressor Gene. *Cancer Discov* **2019**, *9*, 248−263.
(17) D'Assoro, A. B.; Liu, T.; Quatraro, C.; Amato, A.; Opyrchal, M.; Leontovich, A.; Ikeda, Y.; Ohmine, S.; Lingle, W.; Suman, V.; et al. The mitotic kinase Aurora–a promotes distant metastases by inducing epithelial-to-mesenchymal transition in ERalpha(+) breast cancer cells. *Oncogene* **2014**, *33*, 599−610.
(18) Opyrchal, M.; Salisbury, J. L.; Zhang, S.; McCubrey, J.; Hawse, J.; Goetz, M. P.; Lomberk, G. A.; Haddad, T.; Degnim, A.; Lange, C.; et al. Aurora-A mitotic kinase induces endocrine resistance through down-regulation of ERalpha expression in initially ERalpha+ breast cancer cells. *PLoS One* **2014**, *9*, No. e96995.
(19) Otto, T.; Horn, S.; Brockmann, M.; Eilers, U.; Schuttrumpf, L.; Popov, N.; Kenney, A. M.; Schulte, J. H.; Beijersbergen, R.; Christiansen, H.; et al. Stabilization of N-Myc is a critical function of Aurora A in human neuroblastoma. *Cancer Cell* **2009**, *15*, 67−78.
(20) Wu, C.; Lyu, J.; Yang, E. J.; Liu, Y.; Zhang, B.; Shim, J. S. Targeting AURKA-CDC25C axis to induce synthetic lethality in ARID1A-deficient colorectal cancer cells. *Nat. Commun.* **2018**, *9*, 3212.
(21) Ditchfield, C.; Johnson, V. L.; Tighe, A.; Ellston, R.; Haworth, C.; Johnson, T.; Mortlock, A.; Keen, N.; Taylor, S. S. Aurora B couples chromosome alignment with anaphase by targeting BubR1, Mad2, and Cenp-E to kinetochores. *J. Cell Biol.* **2003**, *161*, 267−280.
(22) Nair, J. S.; Ho, A. L.; Tse, A. N.; Coward, J.; Cheema, H.; Ambrosini, G.; Keen, N.; Schwartz, G. K. Aurora B kinase regulates the postmitotic endoreduplication checkpoint via phosphorylation of the retinoblastoma protein at serine 780. *Mol. Biol. Cell* **2009**, *20*, 2218−2228.
(23) Li, Y.; Xu, F. L.; Lu, J.; Saunders, W. S.; Prochownik, E. V. Widespread genomic instability mediated by a pathway involving glycoprotein Ib alpha and Aurora B kinase. *J. Biol. Chem.* **2010**, *285*, 13183−13192.
(24) Coward, J.; Harding, A. Size Does Matter: Why Polyploid Tumor Cells are Critical Drug Targets in the War on Cancer. *Front Oncol* **2014**, *4*, 123.
(25) Bush, T. L.; Payton, M.; Heller, S.; Chung, G.; Hanestad, K.; Rottman, J. B.; Loberg, R.; Friberg, G.; Kendall, R. L.; Saffran, D.; Radinsky, R. AMG 900, a small-molecule inhibitor of aurora kinases, potentiates the activity of microtubule-targeting agents in human metastatic breast cancer models. *Mol. Cancer Ther* **2013**, *12*, 2356−2366.
(26) Carpinelli, P.; Ceruti, R.; Giorgini, M. L.; Cappella, P.; Gianellini, L.; Croci, V.; Degrassi, A.; Texido, G.; Rocchetti, M.; Vianello, P.; et al. PHA-739358, a potent inhibitor of Aurora kinases with a selective target inhibition profile relevant to cancer. *Mol. Cancer Ther* **2007**, *6*, 3158−3168.
(27) Dickson, M. A.; Mahoney, M. R.; Tap, W. D.; D'Angelo, S. P.; Keohan, M. L.; Van Tine, B. A.; Agulnik, M.; Horvath, L. E.; Nair, J. S.; Schwartz, G. K. Phase II study of MLN8237 (Alisertib) in advanced/metastatic sarcoma. *Ann. Oncol* **2016**, *27*, 1855−1860.
(28) Mosse, Y. P.; Fox, E.; Teachey, D. T.; Reid, J. M.; Safgren, S. L.; Carol, H.; Lock, R. B.; Houghton, P. J.; Smith, M. A.; Hall, D.; et al. A Phase II Study of Alisertib in Children with Recurrent/Refractory Solid Tumors or Leukemia: Children's Oncology Group Phase I and Pilot Consortium (ADVL0921). *Clin. Cancer Res.* **2019**, *25*, 3229−3238.
(29) Cohen, J. B.; Maddocks, K. J.; Huang, Y.; Christian, B. A.; Jaglowski, S. M.; Flowers, C. R.; Blum, K. A. A phase 2 trial of alisertib in patients with relapsed or refractory B-cellnon-Hodgkin lymphoma. *Leuk. Lymphoma* **2017**, *58*, 1−2.
(30) O'Connor, O. A.; Ozcan, M.; Jacobsen, E. D.; Roncero, J. M.; Trotman, J.; Demeter, J.; Masszi, T.; Pereira, J.; Ramchandren, R.; Beaven, A.; et al. Randomized Phase III Study of Alisertib or Investigator's Choice (Selected Single Agent) in Patients With Relapsed or Refractory Peripheral T-Cell Lymphoma. *J. Clin Oncol* **2019**, *37*, 613−623.
(31) Vitrac Therapeutics, LLC; Westat. *VIC-1911 Monotherapy in Combination With Sotorasib for the Treatment of KRAS G12C-Mutant Non-Small Cell Lung Cancer*, 2022. https://classic.clinicaltrials.gov/show/NCT05374538.
(32) Jiesi Yingda Pharmaceutical Technology Co., Ltd. *VIC-1911 Combined With Osimertinib for EGFR -Mutant Non-small Cell Lung Cancer*, 2022. https://classic.clinicaltrials.gov/show/NCT05489731.
(33) RenJi Hospital. *Lenvatinib Plus VIC-1911 in Lenvatinib-unresponsive or Lenvatinib-resistant HCC*, 2023. https://classic.clinicaltrials.gov/show/NCT05718882.
(34) Suzhou Junjing BioSciences Co., Ltd.; Sponsor GmbH. *A Study of WJ05129 in Advanced Malignant Solid Tumors*, 2022. https://classic.clinicaltrials.gov/show/NCT05326035.
(35) Eli Lilly and Company; AurKa Pharma Inc. *A Study of AK-01 (LY3295668) in Solid Tumors*, 2017. https://classic.clinicaltrials.gov/show/NCT03092934.
(36) Eli Lilly and Company. *A Study of LY3295668 Erbumine in Participants With Breast Cancer That Has Spread to Other Parts of the Body*, 2019. https://classic.clinicaltrials.gov/show/NCT03955939.
(37) Eli Lilly and Company; NANT; ITCC. *A Study of LY3295668 Erbumine in Participants With Relapsed/Refractory Neuroblastoma*, 2020. https://classic.clinicaltrials.gov/show/NCT04106219.
(38) Littlepage, L. E.; Wu, H.; Andresson, T.; Deanehan, J. K.; Amundadottir, L. T.; Ruderman, J. V. Identification of phosphorylated residues that affect the activity of the mitotic kinase Aurora-A. *Proc. Natl. Acad. Sci. U. S. A.* **2002**, *99*, 15440−15445.
(39) Du, J.; Yan, L.; Torres, R.; Gong, X.; Bian, H.; Marugan, C.; Boehnke, K.; Baquero, C.; Hui, Y. H.; Chapman, S. C.; et al. Aurora A-Selective Inhibitor LY3295668 Leads to Dominant Mitotic Arrest, Apoptosis in Cancer Cells, and Shows Potent Preclinical Antitumor Efficacy. *Mol. Cancer Ther* **2019**, *18*, 2207−2219.
(40) Mou, P. K.; Yang, E. J.; Shi, C.; Ren, G.; Tao, S.; Shim, J. S. Aurora kinase A, a synthetic lethal target for precision cancer medicine. *Exp Mol. Med.* **2021**, *53*, 835−847.
(41) Morel, D.; Almouzni, G.; Soria, J. C.; Postel-Vinay, S. Targeting chromatin defects in selected solid tumors based on oncogene addiction, synthetic lethality and epigenetic antagonism. *Ann. Oncol* **2017**, *28*, 254−269.
(42) Nagarajan, S.; Rao, S. V.; Sutton, J.; Cheeseman, D.; Dunn, S.; Papachristou, E. K.; Prada, J. G.; Couturier, D. L.; Kumar, S.; Kishore, K.; et al. ARID1A influences HDAC1/BRD4 activity, intrinsic proliferative capacity and breast cancer treatment response. *Nat. Genet.* **2020**, *52*, 187−197.
(43) Liu, X.; Li, Z.; Wang, Z.; Liu, F.; Zhang, L.; Ke, J.; Xu, X.; Zhang, Y.; Yuan, Y.; Wei, T.; et al. Chromatin Remodeling Induced by ARID1A Loss in Lung Cancer Promotes Glycolysis and Confers JQ1 Vulnerability. *Cancer Res.* **2022**, *82*, 791−804.
(44) Xu, C.; Huang, K. K.; Law, J. H.; Chua, J. S.; Sheng, T.; Flores, N. M.; Pizzi, M. P.; Okabe, A.; Tan, A. L. K.; Zhu, F.; et al. Comprehensive molecular phenotyping of ARID1A-deficient gastric cancer reveals pervasive epigenomic reprogramming and therapeutic opportunities. *Gut* **2023**, *72*, 1651−1663.
(45) Jacobio Pharmaceuticals Co., Ltd. *A First-in-Human Study of JAB-8263 in Adult Patients With Advanced Solid Tumors*, 2020. https://classic.clinicaltrials.gov/show/NCT04587479.
(46) Jacobio Pharmaceuticals Co., Ltd. *A First-in-Human, JAB-8263 in Adult Patients With Advanced Tumors*, 2021. https://classic.clinicaltrials.gov/show/NCT04686682.
(47) Mollaoglu, G.; Guthrie, M. R.; Bohm, S.; Bragelmann, J.; Can, I.; Ballieu, P. M.; Marx, A.; George, J.; Heinen, C.; Chalishazar, M. D.; et al. MYC Drives Progression of Small Cell Lung Cancer to a Variant Neuroendocrine Subtype with Vulnerability to Aurora Kinase Inhibition. *Cancer Cell* **2017**, *31*, 270−285.
(48) Xu, J.; Chen, Y.; Olopade, O. I. MYC and Breast Cancer. *Genes Cancer* **2010**, *1*, 629−640.
(49) Otte, J.; Dyberg, C.; Pepich, A.; Johnsen, J. I. MYCN Function in Neuroblastoma Development. *Front Oncol* **2021**, *10*, No. 624079.

https://doi.org/10.1021/acsomega.4c01752
ACS Omega 2024, 9, 21416−21425

(50) Peptomy, S.L. *Study to Evaluate the Safety, PK, and Efficacy of the Myc Inhibitor OMO-103 Administered iv in Patients With PDAC*, 2023. https://classic.clinicaltrials.gov/show/NCT06059001.
(51) Harbour, J. W.; Lai, S. L.; Whang-Peng, J.; Gazdar, A. F.; Minna, J. D.; Kaye, F. J. Abnormalities in structure and expression of the human retinoblastoma gene in SCLC. *Science* **1988**, *241*, 353−357.
(52) George, J.; Lim, J. S.; Jang, S. J.; Cun, Y.; Ozretic, L.; Kong, G.; Leenders, F.; Lu, X.; Fernandez-Cuesta, L.; Bosco, G.; et al. Comprehensive genomic profiles of small cell lung cancer. *Nature* **2015**, *524*, 47−53.
(53) Jacobio Pharmaceuticals Co., Ltd. *JAB-2485 Activity in Adult Patients With Advanced Solid Tumors*, 2022. https://classic.clinicaltrials.gov/show/NCT05490472.
(54) Trigo, J.; Subbiah, V.; Besse, B.; Moreno, V.; Lopez, R.; Sala, M. A.; Peters, S.; Ponce, S.; Fernandez, C.; Alfaro, V.; et al. Lurbinectedin as second-line treatment for patients with small-cell lung cancer: a single-arm, open-label, phase 2 basket trial. *Lancet Oncol* **2020**, *21*, 645−654.
(55) Owonikoko, T. K.; Niu, H.; Nackaerts, K.; Csoszi, T.; Ostoros, G.; Mark, Z.; Baik, C.; Joy, A. A.; Chouaid, C.; Jaime, J. C.; et al. Randomized Phase II Study of Paclitaxel plus Alisertib versus Paclitaxel plus Placebo as Second-Line Therapy for SCLC: Primary and Correlative Biomarker Analyses. *J. Thorac Oncol* **2020**, *15*, 274−287.
(56) Ariey-Bonnet, J.; Berges, R.; Montero, M. P.; Mouysset, B.; Piris, P.; Muller, K.; Pinna, G.; Failes, T. W.; Arndt, G. M.; Morando, P.; et al. Combination drug screen targeting glioblastoma core vulnerabilities reveals pharmacological synergisms. *EBioMedicine* **2023**, *95*, No. 104752.
(57) Yi, J. S.; Sias-Garcia, O.; Nasholm, N.; Hu, X.; Iniguez, A. B.; Hall, M. D.; Davis, M.; Guha, R.; Moreno-Smith, M.; Barbieri, E.; et al. The synergy of BET inhibitors with aurora A kinase inhibitors in MYCN-amplified neuroblastoma is heightened with functional TP53. *Neoplasia* **2021**, *23*, 624−633.
(58) Sahni, J. M.; Gayle, S. S.; Bonk, K. L.; Vite, L. C.; Yori, J. L.; Webb, B.; Ramos, E. K.; Seachrist, D. D.; Landis, M. D.; Chang, J. C.; et al. Bromodomain and Extraterminal Protein Inhibition Blocks Growth of Triple-negative Breast Cancers through the Suppression of Aurora Kinases. *J. Biol. Chem.* **2016**, *291*, 23756−23768.

https://doi.org/10.1021/acsomega.4c01752
ACS Omega 2024, 9, 21416−21425